Acta Cryst E CRYSTALLOGRAPHIC COMMUNICATIONS
ISSN 2056-9890

Synthesis, crystal structure and properties of bis(isoselenocyanato-κN)tetrakis(pyridine-κN)-nickel(II)

Christian Näther* and Jan Boeckmann

Institut für Anorganische Chemie, Universität Kiel, Max-Eyth-Str. 2, 24118 Kiel, Germany. *Correspondence e-mail: cnaether@ac.uni-kiel.de

Received 6 January 2023
Accepted 10 January 2023

Edited by W. T. A. Harrison, University of Aberdeen, United Kingdom

Keywords: crystal structure; nickel selenocyanate; discrete complex; thermal properties.

CCDC reference: 2235328

Supporting information: this article has supporting information at journals.iucr.org/e

The reaction of nickel chloride hexahydrate with potassium selenocyanate and pyridine in water leads to the formation of crystals of the title complex, $[Ni(NCSe)_2(C_5H_5N)_4]$, which were characterized by single-crystal X-ray diffraction. Its crystal structure consists of discrete complexes, located on centers of inversion, in which the Ni cations are sixfold coordinated by two terminal N-bonded selenocyanate anions and four pyridine ligands within a slightly distorted octahedral coordination. In the crystal, the complexes are connected by weak C—H···Se interactions. PXRD investigations revealed that a pure crystalline phase has formed. In the IR and Raman spectra, the C—N stretching vibrations are observed at 2083 and 2079 cm^{-1}, respectively, in agreement with the presence of only terminally bonded anionic ligands. Upon heating, one well-resolved mass loss is observed, in which two of the four pyridine ligands are removed, leading to a compound with the composition $Ni(NCSe)_2(C_5H_5N)_2$. In this compound, the C—N stretching vibration is shifted to 2108 cm^{-1} (Raman) and 2115 cm^{-1} (IR), indicating the presence of μ-1,3-bridging anionic ligands. In its PXRD pattern, very broad reflections are observed, indicating for poor crystallinity and/or very small particle size. This crystalline phase is not isotypic to its Co and Fe analogs.

1. Chemical context

Coordination compounds based on thiocanate anions are well investigated, which can partly be traced back to their versatile magnetic behavior, including antiferro- or ferromagnetic ordering as well as single-chain magnet behavior (Shurdha *et al.*, 2013; Prananto *et al.*, 2017; Mautner *et al.*, 2018; Werner *et al.*, 2014; Rams *et al.*, 2020). In contrast, much less is known about the corresponding selenocyanate coordination compounds, which might be related to the fact that their synthesis is more difficult to achieve. This is especially the case if less chalcophilic metal cations are used and compounds with bridging anionic ligands are to be prepared. Therefore, only a very limited number of such compounds have been reported in the literature (Turpeinen, 1977; Vicente *et al.*, 1993; Wöhlert *et al.*, 2012). To overcome this problem, we developed a synthetic procedure that allows a more directed preparation of thio- and selenocyanate coordination compounds with bridging anionic ligands, which is based on thermal treatment of suitable precursor compounds in which the anionic ligands are only terminally bonded (Werner *et al.*, 2015; Wriedt & Näther, 2010). Upon heating, the neutral coligands are usually stepwise removed, leading to the formation of the desired compounds with a bridging coordination as intermediates.

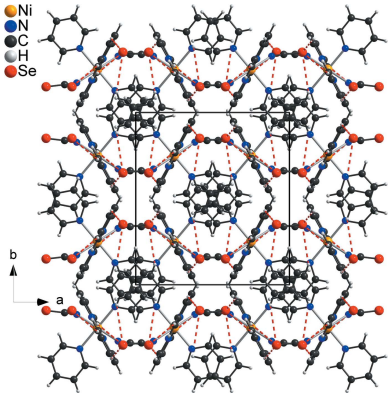

This procedure works perfectly for the synthesis of thiocyanates but can also be used for the synthesis of selenocyanates (Wöhlert *et al.*, 2012).

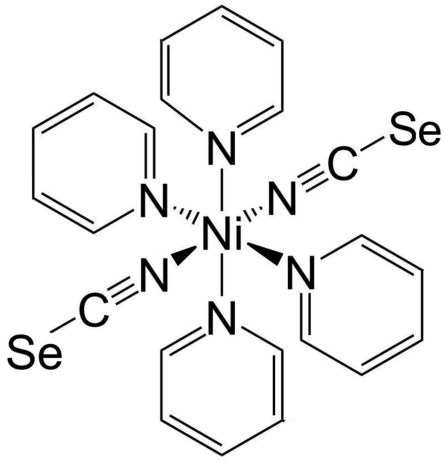

In this context we have reported on compounds with the composition $M(NCSe)_2(pyridine)_4$ (M = Fe, Co) that upon heating lose two of the pyridine coligands and transform into compounds with the composition $M(NCSe)_2(pyridine)_2$ (M = Fe, Co), in which the metal cations are linked by pairs of μ-1,3-bridging selenocyanate anions into chains (Boeckmann *et al.*, 2012; Boeckmann & Näther, 2011). In the course of our systematic work we also became interested in the corresponding Ni compounds, which are not reported in the literature. The synthesis of the desired compound $Ni(NCSe)_2(pyridine)_2$ in solution was unsuccessful but we found that single crystals, as well as larger amounts of a microcrystalline powder with the composition $Ni(NCSe)_2(pyridine)_4$, can easily be prepared from solution. The CN stretching vibrations of the anionic ligand are observed at 2083 cm^{-1} in the IR and at 2079 cm^{-1} in the Raman spectrum, which indicates that the selenocyanate anions are only terminally bonded (Fig. S1 in the supporting information). A comparison of the experimental powder X-ray pattern with that calculated from single-crystal data reveals that a pure crystalline phase has formed (Fig. 1). Measurements using differential thermal analysis and thermogravimetry coupled to mass spectrometry (DTA–TG–MS) show one well-resolved mass loss in which the pyridine ligands are emitted and that is accompanied with an endothermic event in the DTA curve at 140°C (Fig. 2). Upon further heating, the TG curve is poorly resolved and two additionally endothermic events are observed. The experimental mass loss of 26.4% in the first step is close to that calculated for the removal of half of the pyridine ligands (27.0%). Therefore, it can be assumed that in the first mass loss a compound with the composition $Ni(NCS)_2(pyridine)_2$ is formed that, upon further heating, loses the remaining pyridine ligands and that this event cannot be separated from the decomposition of nickel selenocyanate at higher temperatures. For this residue, IR and Raman spectroscopy show that the CN stretching vibrations are located at 2115 cm^{-1} in the IR and at 2108 cm^{-1} in the Raman spectrum, indicating that μ-1,3-bridging selenocyanate anions are present (Fig. S2).

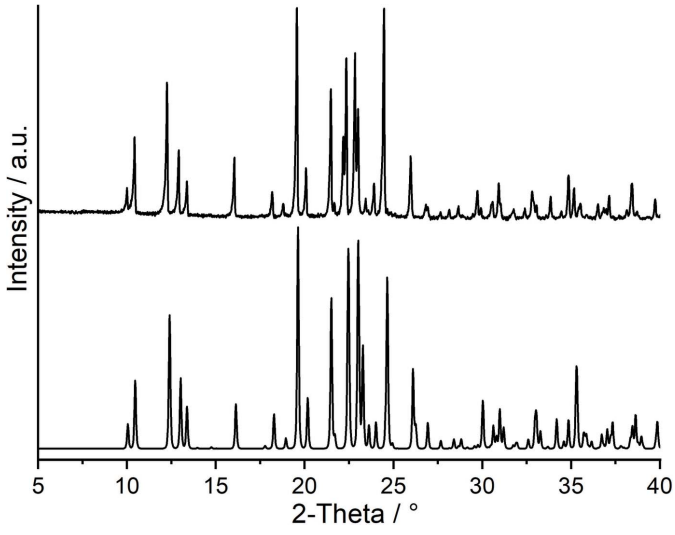

Figure 1
Experimental (top) and calculated PXRD pattern (bottom) of the title compound.

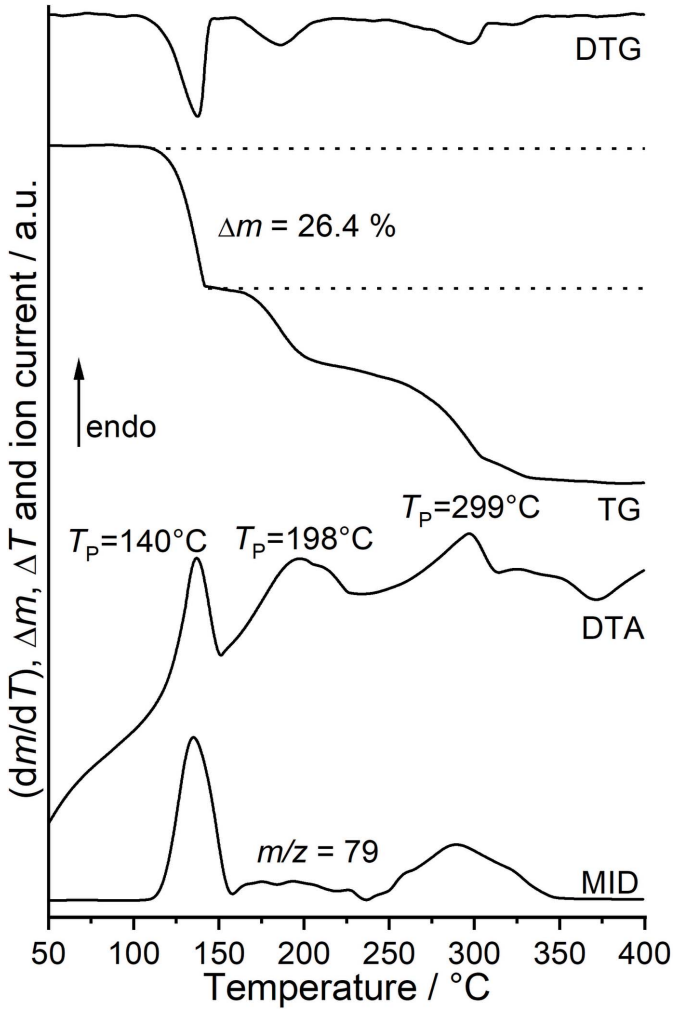

Figure 2
DTG, TG, DTA and MS trend scan curves for the title compound measured at 4°C min^{-1} in helium.

Table 1
Selected geometric parameters (Å, °).

Ni1—N1	2.061 (2)	Ni1—N21	2.165 (2)
Ni1—N11	2.159 (2)		
N1^{i}—Ni1—N1	180.0	N1^{i}—Ni1—N21	90.75 (9)
N1^{i}—Ni1—N11	91.10 (9)	N1—Ni1—N21	89.25 (9)
N1—Ni1—N11	88.90 (9)	N11—Ni1—N21	92.40 (8)

Symmetry code: (i) $-x+\frac{3}{2}, -y+\frac{3}{2}, -z+1$.

PXRD investigations proved that the reflections of the precursor compound are absent but that a residue of poor crystallinity and/or very small particle size is obtained (Fig. S3). A comparison of the experimental powder pattern with that calculated for $Co(NCSe)_2(pyridine)_2$ retrieved from literature shows that these compounds are not isotypic (Fig. S3). Indexing of this powder pattern failed.

2. Structural commentary

Single-crystal structure determination proves that the title compound, $Ni(NCSe)_2(pyridine)_4$, is isotypic to its Co, Fe, Cd and Zn analogs already described in the literature (Boeckmann & Näther, 2011; Boeckmann *et al.*, 2011 and 2012). The asymmetric unit consists of one crystallographically independent Ni^{II} cation that is located on a center of inversion as well as one selenocyanate anion and two pyridine ligands in a general position (Fig. 3). The Ni cations are sixfold coordinated by four pyridine coligands and two terminally N-bonded selenocyanate anions in *trans*-positions. Bond lengths are similar to those in the corresponding Fe and Co compounds, even if the Ni—N bond lengths are slightly shortened because of the lower ionic radii. From the bond lengths and angles (Table 1) it is obvious that the octahedra are slightly distorted.

Table 2
Hydrogen-bond geometry (Å, °).

D—H···*A*	*D*—H	H···*A*	*D*···*A*	*D*—H···*A*
C11—H11···Se1^{ii}	0.95	3.09	3.895 (3)	144
C11—H11···N1^{i}	0.95	2.67	3.173 (4)	114
C12—H12···Se1^{iii}	0.95	3.11	3.972 (3)	151
C15—H15···N1	0.95	2.60	3.074 (4)	111
C21—H21···N1	0.95	2.54	3.061 (4)	115
C22—H22···Se1^{iv}	0.95	3.13	4.022 (3)	157
C25—H25···Se1^{ii}	0.95	3.00	3.725 (3)	134
C25—H25···N1^{i}	0.95	2.55	3.103 (4)	118

Symmetry codes: (i) $-x+\frac{3}{2}, -y+\frac{3}{2}, -z+1$; (ii) $x+\frac{1}{2}, y-\frac{1}{2}, z$; (iii) $-x+1, -y+1, -z+1$; (iv) $-x+1, y, -z+\frac{3}{2}$.

3. Supramolecular features

In the crystal, the $Ni(NCSe)_2$ units are arranged in corrugated layers in the *ac* plane and the pyridine rings are arranged in columns that proceed along the crystallographic *c*-axis direction with no sign of π–π interactions (Fig. 4). There are some C—H···Se contacts, with angles above 150°, indicating weak hydrogen-bonding interactions (Table 2). There are additional C—H···N contacts, but distances and especially angles indicate that they should not correspond to any significant interactions (Table 2).

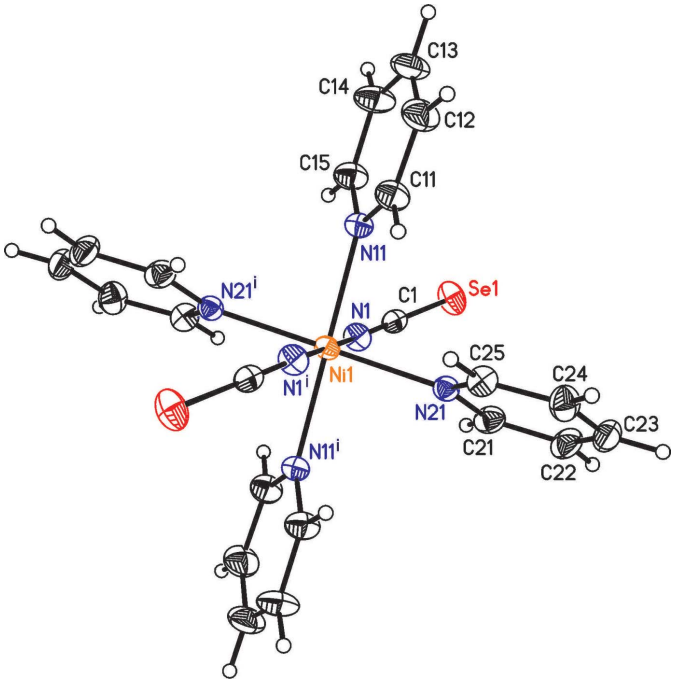

Figure 3
Crystal structure of the title compound with labeling and displacement ellipsoids drawn at the 50% probability level. Symmetry code: (i) $-x+\frac{3}{2}, -y+\frac{3}{2}, -z+1$.

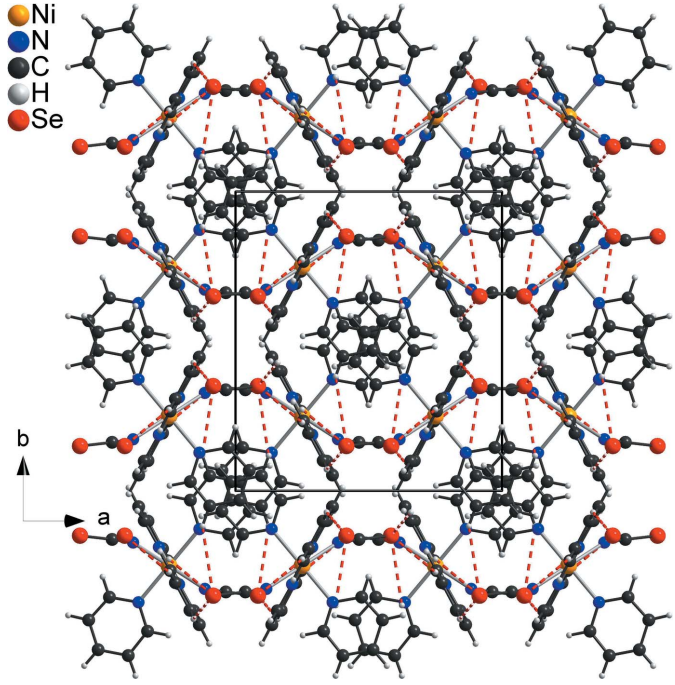

Figure 4
Crystal structure of the title compound with view along the crystallographic *c*-axis direction. C—H···Se interactions are shown as red dashed lines.

Table 3
Experimental details.

Crystal data	
Chemical formula	$[Ni(NCSe)_2(C_5H_5N)_4]$
M_r	585.07
Crystal system, space group	Monoclinic, *C*2/*c*
Temperature (K)	170
a, *b*, *c* (Å)	12.4422 (10), 13.2302 (9), 15.0723 (12)
β (°)	108.755 (9)
V (Å^3)	2349.4 (3)
Z	4
Radiation type	Mo $K\alpha$
μ (mm^{-1})	3.95
Crystal size (mm)	0.50 × 0.40 × 0.30
Data collection	
Diffractometer	Stoe *IPDS2*
Absorption correction	Numerical (*X-SHAPE* and *X-RED* 32; Stoe, 2008)
T_{min}, T_{max}	0.486, 0.563
No. of measured, independent and observed [$I > 2\sigma(I)$] reflections	7129, 2485, 1971
R_{int}	0.034
(sin $\theta/\lambda)_{max}$ (Å^{-1})	0.639
Refinement	
$R[F^2 > 2\sigma(F^2)]$, $wR(F^2)$, S	0.030, 0.075, 1.02
No. of reflections	2485
No. of parameters	142
H-atom treatment	H-atom parameters constrained
$\Delta\rho_{max}$, $\Delta\rho_{min}$ (e Å^{-3})	0.89, −0.64

Computer programs: *X-AREA* (Stoe, 2008), *SHELXT2014/5* (Sheldrick, 2015*a*), *SHELXL2016/6* (Sheldrick, 2015*b*), *DIAMOND* (Brandenburg & Putz, 1999) and *publCIF* (Westrip, 2010).

4. Database survey

Some selenocyanate compounds with pyridine as ligand have been deposited in the Cambridge Structural Database [ConQuest Version 2022.2.0, CSD Version 5.43 (March 2022); Groom *et al.*, 2016], including isotypic compounds with composition $M(NCSe)_2(pyridine)_4$ (M = Co, Fe, Cd, Zn) in which the metal cations are octahedrally coordinated by two terminal N-bonded selenocyanate anions and four pyridine ligands (refcodes ITISOU, CAQVEX, OWOJAM and OWOHUE; Boeckmann & Näther, 2011; Boeckmann *et al.*, 2012, 2011). For these compounds, mixed crystals with the composition $Co(NCS)_x(NCSe)_{2-x}(pyridine)_4$ have also been reported (refcodes TIXDOW and TIXDOW01; Neumann *et al.*, 2019).

There are compounds with the composition $M(NCSe)_2(pyridine)_2$ (M = Co, Fe, Cd) in which the metal cations are octahedrally coordinated by two terminal N- and S-bonded selenocyanate anions and two pyridine ligands and are linked by pairs of selenocyanate anions into chains (refcodes: ITISUA, CAQVIB and OWOHOY; Boeckmann & Näther, 2011; Boeckmann *et al.*, 2012, 2011). These compounds are also isotypic. There is an additional compound of composition $Zn(NCSe)_2(pyridine)_2$ that consists of discrete complexes in which the Zn cations are tetrahedrally coordinated by two terminal N-bonded selenocyanate anions and two pyridine ligands (refcode OWOJEQ; Boeckmann *et al.*, 2011).

One mixed-metal compound with the composition $HgSr(NCSe)_4(pyridine)_6$ is also reported, in which the Hg cations are tetrahedrally coordinated by four Se-bonded selenocyanate anions and linked to the Sr cations that are octahedrally coordinated by two N-bonded selenocyanate anions and four pyridine ligands (refcode CICLOP; Brodersen *et al.*, 1984).

A dinuclear complex with the composition $(Fe(NCS)_2)_2(pyridine)_2$((3,5-bis(pyridin-2-yl)pyrazolyl)$_2$ is found that shows spin-crossover behavior (refcode FIZYEU; Sy *et al.*, 2014). Finally, there is another spin-crossover complex with the composition $Fe(NCSe)_2(pyridine)_2$-2-methyldipyrido-[3,2-*f*:2′,3′-*h*](quinoxaline) pyridine solvate (refcode TISWOI; Tao *et al.*, 2007).

5. Synthesis and crystallization

$NiCl_2{\cdot}6H_2O$ and $K(SeCN)_2$ were purchased from Merck and pyridine was purchased from Alfa Aesar.

Synthesis:

Larger amounts of a microcrystalline powder were obtained by the reaction of 59.4 mg of $NiCl_2{\cdot}6H_2O$ (0.25 mmol) and 72.0 mg (0.5 mmol) of KSeCN in a mixture of 1.5 ml of pyridine and 1.5 ml of water by stirring for 3 d at room temperature. The precipitate was filtered off and washed with a very small amount of water. Single crystals in the form of purple blocks were obtained under the same conditions but without stirring.

Experimental details:

Differential thermal analysis and thermogravimetric (DTA–TG–MS) measurements were performed in a dynamic helium atmosphere in Al_2O_3 crucibles using a Netzsch thermobalance with skimmer coupling and a Balzer Quadrupol MS. The XRPD measurements were performed by using a Stoe Transmission Powder Diffraction System (STADI P) equipped with a linear, position-sensitive MYTHEN detector from Stoe & Cie with Cu $K\alpha$ radiation. The IR data were measured using a Bruker Alpha-P ATR-IR spectrometer and the Raman spectra were measured with a Bruker Vertex 70 spectrometer.

6. Refinement

Crystal data, data collection and structure refinement details are summarized in Table 3. Hydrogen atoms were positioned with idealized geometry (C—H = 0.95 Å) and were refined with U_{iso}(H) = 1.2U_{eq}(C) using a riding model.

Acknowledgements

This work was supported by the state of Schleswig-Holstein.

References

Boeckmann, J. & Näther, C. (2011). *Chem. Commun.* **47**, 7104–7106.
Boeckmann, J., Reinert, T. & Näther, C. (2011). *Z. Anorg. Allg. Chem.* **637**, 940–946.
Boeckmann, J., Wriedt, M. & Näther, C. (2012). *Chem. Eur. J.* **18**, 5284–5289.

Brandenburg, K. & Putz, H. (1999). *DIAMOND*. Crystal Impact GbR, Bonn, Germany.

Brodersen, K., Cygan, M. & Hummel, H. U. (1984). *Z. Naturforsch. Teil B*, **39**, 2582–585.

Groom, C. R., Bruno, I. J., Lightfoot, M. P. & Ward, S. C. (2016). *Acta Cryst*. B**72**, 171–179.

Mautner, F. A., Traber, M., Fischer, R. C., Torvisco, A., Reichmann, K., Speed, S., Vicente, R. & Massoud, S. S. (2018). *Polyhedron*, **154**, 436–442.

Neumann, T., Rams, M., Tomkowicz, Z., Jess, I. & Näther, C. (2019). *Chem. Commun.* **55**, 2652–2655.

Prananto, Y. P., Urbatsch, A., Moubaraki, B., Murray, K. S., Turner, D. R., Deacon, G. B. & Batten, S. R. (2017). *Aust. J. Chem.* **70**, 516–528.

Rams, M., Jochim, A., Böhme, M., Lohmiller, T., Ceglarska, M., Rams, M. M., Schnegg, A., Plass, W. & Näther, C. (2020). *Chem. Eur. J.* **26**, 2837–2851.

Sheldrick, G. M. (2015*a*). *Acta Cryst.* A**71**, 3–8.

Sheldrick, G. M. (2015*b*). *Acta Cryst.* C**71**, 3–8.

Shurdha, E., Moore, C. E., Rheingold, A. L., Lapidus, S. H., Stephens, P. W., Arif, A. M. & Miller, J. S. (2013). *Inorg. Chem.* **52**, 10583–10594.

Stoe (2008). *X-AREA*, *X-RED32* and *X-SHAPE*. Stoe & Cie, Darmstadt, Germany.

Sy, M., Varret, F., Boukheddaden, K., Bouchez, G., Marrot, S., Kawata, S. & Kaizaki, S. (2014). *Angew. Chem. Int. Ed.* **53**, 7539–7542.

Tao, J. Q., Gu, Z. G., Wang, T. W., Yang, Q. F., Zuo, J. L. & You, X. Z. (2007). *Inorg. Chim. Acta*, **360**, 4125–4132.

Turpeinen, U. (1977). *Finn. Chem. Lett.* **3**, 75–78.

Vicente, R., Escuer, A., Ribas, J., Solans, X. & Font-Bardia, M. (1993). *Inorg. Chem.* **32**, 6117–6118.

Werner, J., Rams, M., Tomkowicz, Z. & Näther, C. (2014). *Dalton Trans.* **43**, 17333–17342.

Werner, J., Runčevski, T., Dinnebier, R., Ebbinghaus, S. G., Suckert, S. & Näther, C. (2015). *Eur. J. Inorg. Chem.* **2015**, 3236–3245.

Westrip, S. P. (2010). *J. Appl. Cryst.* **43**, 920–925.

Wöhlert, S., Ruschewitz, U. & Näther, C. (2012). *Cryst. Growth Des.* **12**, 2715–2718.

Wriedt, M. & Näther, C. (2010). *Chem. Commun.* **46**, 4707–4709.

supporting information

Acta Cryst. (2023). E**79**, 90-94 [https://doi.org/10.1107/S2056989023000245]

Synthesis, crystal structure and properties of bis(isoselenocyanato-κ*N*)tetrakis-(pyridine-κ*N*)nickel(II)

Christian Näther and Jan Boeckmann

Computing details

Data collection: *X-AREA* (Stoe, 2008); cell refinement: *X-AREA* (Stoe, 2008); data reduction: *X-AREA* (Stoe, 2008); program(s) used to solve structure: *SHELXT2014/5* (Sheldrick, 2015a); program(s) used to refine structure: *SHELXL2016/6* (Sheldrick, 2015b); molecular graphics: *DIAMOND* (Brandenburg & Putz, 1999); software used to prepare material for publication: *publCIF* (Westrip, 2010).

Bis(isoselenocyanato-κ*N*)tetrakis(pyridine-κ*N*)nickel(II)

Crystal data

$[Ni(NCSe)_2(C_5H_5N)_4]$
M_r = 585.07
Monoclinic, *C*2/*c*
a = 12.4422 (10) Å
b = 13.2302 (9) Å
c = 15.0723 (12) Å
β = 108.755 (9)°
V = 2349.4 (3) Å^3
Z = 4
F(000) = 1160
D_x = 1.654 Mg m^{-3}
Mo *Kα* radiation, *λ* = 0.71073 Å
Cell parameters from 7129 reflections
θ = 2.3–27.0°
μ = 3.95 mm^{-1}
T = 170 K
Block, purple
0.50 × 0.40 × 0.30 mm

Data collection

Stoe IPDS-2 diffractometer
ω scans
Absorption correction: numerical (X-Shape and X-Red 32; Stoe, 2008)
T_{min} = 0.486, T_{max} = 0.563
7129 measured reflections
2485 independent reflections
1971 reflections with $I > 2\sigma(I)$
R_{int} = 0.034
θ_{max} = 27.0°, θ_{min} = 2.3°
h = −15→15
k = −13→16
l = −19→19

Refinement

Refinement on F^2
Least-squares matrix: full
$R[F^2 > 2\sigma(F^2)]$ = 0.030
$wR(F^2)$ = 0.075
S = 1.02
2485 reflections
142 parameters
0 restraints
Primary atom site location: dual
Hydrogen site location: inferred from neighbouring sites
H-atom parameters constrained
$w = 1/[\sigma^2(F_o^2) + (0.0461P)^2]$ where $P = (F_o^2 + 2F_c^2)/3$
$(\Delta/\sigma)_{max} < 0.001$
$\Delta\rho_{max}$ = 0.89 e Å^{-3}
$\Delta\rho_{min}$ = −0.64 e Å^{-3}

Special details

Geometry. All esds (except the esd in the dihedral angle between two l.s. planes) are estimated using the full covariance matrix. The cell esds are taken into account individually in the estimation of esds in distances, angles and torsion angles; correlations between esds in cell parameters are only used when they are defined by crystal symmetry. An approximate (isotropic) treatment of cell esds is used for estimating esds involving l.s. planes.

Fractional atomic coordinates and isotropic or equivalent isotropic displacement parameters (Å²)

	x	*y*	*z*	U_{iso}*/U_{eq}
Ni1	0.750000	0.750000	0.500000	0.01661 (12)
N11	0.63560 (19)	0.62770 (17)	0.43798 (16)	0.0204 (5)
C11	0.6697 (3)	0.5310 (2)	0.4492 (2)	0.0277 (6)
H11	0.747512	0.517340	0.481265	0.033*
C12	0.5971 (3)	0.4497 (3)	0.4165 (2)	0.0365 (7)
H12	0.624361	0.382260	0.427221	0.044*
C13	0.4841 (3)	0.4692 (3)	0.3678 (2)	0.0397 (8)
H13	0.432159	0.415397	0.344311	0.048*
C14	0.4487 (3)	0.5685 (3)	0.3543 (3)	0.0391 (8)
H14	0.371805	0.584215	0.320745	0.047*
C15	0.5265 (3)	0.6448 (2)	0.3902 (2)	0.0291 (6)
H15	0.501079	0.712884	0.380325	0.035*
N21	0.78775 (18)	0.68763 (17)	0.63947 (15)	0.0193 (5)
C21	0.7547 (2)	0.7336 (2)	0.7063 (2)	0.0258 (6)
H21	0.716401	0.796653	0.692048	0.031*
C22	0.7742 (3)	0.6931 (3)	0.7948 (2)	0.0312 (7)
H22	0.750093	0.728412	0.839944	0.037*
C23	0.8288 (3)	0.6010 (3)	0.8172 (2)	0.0319 (7)
H23	0.842008	0.571618	0.877261	0.038*
C24	0.8638 (3)	0.5528 (2)	0.7495 (2)	0.0299 (6)
H24	0.901305	0.489356	0.762043	0.036*
C25	0.8428 (2)	0.5993 (2)	0.6628 (2)	0.0244 (6)
H25	0.868951	0.566730	0.617400	0.029*
Se1	0.41596 (3)	0.85023 (2)	0.58223 (2)	0.02991 (11)
C1	0.5366 (2)	0.83774 (19)	0.54277 (18)	0.0196 (5)
N1	0.6154 (2)	0.82749 (18)	0.51901 (16)	0.0228 (5)

Atomic displacement parameters (Å²)

	U^{11}	U^{22}	U^{33}	U^{12}	U^{13}	U^{23}
Ni1	0.0135 (2)	0.0166 (2)	0.0203 (2)	0.00038 (17)	0.0062 (2)	−0.00075 (18)
N11	0.0182 (12)	0.0201 (12)	0.0227 (11)	−0.0014 (9)	0.0061 (10)	−0.0024 (9)
C11	0.0268 (16)	0.0216 (15)	0.0342 (16)	0.0006 (12)	0.0090 (14)	−0.0016 (12)
C12	0.044 (2)	0.0225 (15)	0.0430 (18)	−0.0059 (14)	0.0145 (17)	−0.0052 (14)
C13	0.041 (2)	0.0353 (19)	0.0436 (19)	−0.0199 (15)	0.0143 (17)	−0.0140 (15)
C14	0.0221 (17)	0.041 (2)	0.046 (2)	−0.0095 (13)	0.0004 (16)	−0.0070 (16)
C15	0.0228 (16)	0.0275 (15)	0.0333 (16)	−0.0016 (12)	0.0038 (14)	−0.0019 (12)
N21	0.0173 (12)	0.0204 (11)	0.0201 (11)	−0.0011 (9)	0.0061 (10)	−0.0006 (9)
C21	0.0231 (15)	0.0300 (15)	0.0244 (14)	−0.0004 (11)	0.0078 (13)	−0.0056 (12)

C22	0.0315 (17)	0.0428 (18)	0.0207 (13)	−0.0025 (14)	0.0103 (14)	−0.0067 (13)
C23	0.0279 (17)	0.047 (2)	0.0198 (14)	−0.0048 (14)	0.0059 (14)	0.0037 (13)
C24	0.0295 (16)	0.0296 (16)	0.0301 (14)	0.0048 (13)	0.0088 (14)	0.0073 (13)
C25	0.0242 (16)	0.0243 (15)	0.0249 (14)	0.0029 (11)	0.0079 (13)	−0.0008 (11)
Se1	0.02946 (18)	0.02786 (17)	0.04138 (19)	0.00354 (12)	0.02390 (15)	0.00093 (13)
C1	0.0225 (14)	0.0150 (12)	0.0186 (13)	0.0024 (10)	0.0028 (12)	−0.0001 (10)
N1	0.0186 (12)	0.0235 (12)	0.0270 (12)	0.0028 (9)	0.0084 (11)	0.0007 (9)

Geometric parameters (Å, º)

Ni1—N1^{i}	2.061 (2)	C14—H14	0.9500
Ni1—N1	2.061 (2)	C15—H15	0.9500
Ni1—N11	2.159 (2)	N21—C25	1.342 (4)
Ni1—N11^{i}	2.159 (2)	N21—C21	1.350 (3)
Ni1—N21	2.165 (2)	C21—C22	1.384 (4)
Ni1—N21^{i}	2.165 (2)	C21—H21	0.9500
N11—C15	1.336 (4)	C22—C23	1.383 (5)
N11—C11	1.342 (4)	C22—H22	0.9500
C11—C12	1.388 (4)	C23—C24	1.387 (4)
C11—H11	0.9500	C23—H23	0.9500
C12—C13	1.385 (5)	C24—C25	1.391 (4)
C12—H12	0.9500	C24—H24	0.9500
C13—C14	1.380 (5)	C25—H25	0.9500
C13—H13	0.9500	Se1—C1	1.792 (3)
C14—C15	1.384 (4)	C1—N1	1.154 (3)
N1^{i}—Ni1—N1	180.0	C13—C14—C15	119.1 (3)
N1^{i}—Ni1—N11	91.10 (9)	C13—C14—H14	120.4
N1—Ni1—N11	88.90 (9)	C15—C14—H14	120.4
N1^{i}—Ni1—N11^{i}	88.90 (9)	N11—C15—C14	123.3 (3)
N1—Ni1—N11^{i}	91.10 (9)	N11—C15—H15	118.3
N11—Ni1—N11^{i}	180.00 (8)	C14—C15—H15	118.3
N1^{i}—Ni1—N21	90.75 (9)	C25—N21—C21	116.7 (2)
N1—Ni1—N21	89.25 (9)	C25—N21—Ni1	121.25 (17)
N11—Ni1—N21	92.40 (8)	C21—N21—Ni1	122.01 (19)
N11^{i}—Ni1—N21	87.60 (8)	N21—C21—C22	122.9 (3)
N1^{i}—Ni1—N21^{i}	89.25 (9)	N21—C21—H21	118.5
N1—Ni1—N21^{i}	90.75 (9)	C22—C21—H21	118.5
N11—Ni1—N21^{i}	87.61 (8)	C23—C22—C21	119.8 (3)
N11^{i}—Ni1—N21^{i}	92.40 (8)	C23—C22—H22	120.1
N21—Ni1—N21^{i}	180.0	C21—C22—H22	120.1
C15—N11—C11	117.1 (3)	C22—C23—C24	118.1 (3)
C15—N11—Ni1	121.4 (2)	C22—C23—H23	120.9
C11—N11—Ni1	121.5 (2)	C24—C23—H23	120.9
N11—C11—C12	123.4 (3)	C23—C24—C25	118.7 (3)
N11—C11—H11	118.3	C23—C24—H24	120.7
C12—C11—H11	118.3	C25—C24—H24	120.7
C13—C12—C11	118.5 (3)	N21—C25—C24	123.8 (3)

C13—C12—H12	120.7	N21—C25—H25	118.1
C11—C12—H12	120.7	C24—C25—H25	118.1
C14—C13—C12	118.5 (3)	N1—C1—Se1	178.1 (2)
C14—C13—H13	120.8	C1—N1—Ni1	155.6 (2)
C12—C13—H13	120.8		

Symmetry code: (i) −*x*+3/2, −*y*+3/2, −*z*+1.

Hydrogen-bond geometry (Å, º)

D—H···*A*	*D*—H	H···*A*	*D*···*A*	*D*—H···*A*
C11—H11···Se1^{ii}	0.95	3.09	3.895 (3)	144
C11—H11···N1^{i}	0.95	2.67	3.173 (4)	114
C12—H12···Se1^{iii}	0.95	3.11	3.972 (3)	151
C15—H15···N1	0.95	2.60	3.074 (4)	111
C21—H21···N1	0.95	2.54	3.061 (4)	115
C22—H22···Se1^{iv}	0.95	3.13	4.022 (3)	157
C25—H25···Se1^{ii}	0.95	3.00	3.725 (3)	134
C25—H25···N1^{i}	0.95	2.55	3.103 (4)	118

Symmetry codes: (i) −*x*+3/2, −*y*+3/2, −*z*+1; (ii) *x*+1/2, *y*−1/2, *z*; (iii) −*x*+1, −*y*+1, −*z*+1; (iv) −*x*+1, *y*, −*z*+3/2.